Integrated genetic, epigenetic, and immune landscape of *TP53* mutant AML and higher risk MDS treated with azacitidine

Amer M. Zeidan[1]*[iD], **Jan Philipp Bewersdorf**[1,2]*[iD], **Vanessa Hasle**[3], **Rory M. Shallis**[1][iD], **Ethan Thompson**[3], **Daniel Lopes de Menezes**[3], **Shelonidta Rose**[3], **Isaac Boss**[3], **Stephanie Halene**[1], **Torsten Haferlach**[4] and **Brian A. Fox**[3]

Abstract

Background: *TP53* mutations are associated with an adverse prognosis in acute myeloid leukemia (AML) and higher-risk myelodysplastic syndromes (HR-MDS). However, the integrated genetic, epigenetic, and immunologic landscape of *TP53*-mutated AML/HR-MDS is not well defined.

Objectives: To define the genetic, epigenetic, and immunologic landscape of *TP53*-mutant and *TP53* wild-type AML and HR-MDS patients.

Design: *Post hoc* analysis of *TP53*-mutant and *TP53* wild-type patients treated on the randomized FUSION trial with azacitidine ± the anti-PD-L1 antibody durvalumab.

Methods: We performed extensive molecular, epigenetic, and immunologic assays on a well-annotated clinical trial dataset of 61 patients with *TP53*-mutated disease (37 AML, 24 MDS) and 144 *TP53* wild-type (89 AML, 55 MDS) patients, all of whom received azacitidine-based therapy. A 38 gene-targeted myeloid mutation analysis from screening bone marrow (BM) was performed. DNA methylation arrays, immunophenotyping and immune checkpoint expression by flow cytometry, and gene expression profiles by bulk RNA sequencing were assessed at baseline and serially during the trial.

Results: Global DNA methylation from peripheral blood was independent of *TP53* mutation and allelic status. AZA therapy led to a statistically significant decrease in global DNA methylation scores independent of *TP53* mutation status. In BM from *TP53*-mutant patients, we found both a higher T-cell population and upregulation of inhibitory immune checkpoint proteins such as PD-L1 compared to *TP53* wild-type. RNA sequencing analyses revealed higher expression of the myeloid immune checkpoint gene *LILRB3* in *TP53*-mutant samples suggesting a novel therapeutic target.

Conclusion: This integrated analysis of the genetic, epigenetic, and immunophenotypic landscape of *TP53* mutant AML/HR-MDS suggests that differences in the immune landscape resulting in an immunosuppressive microenvironment rather than epigenetic differences contribute to the poor prognosis of *TP53*-mutant AML/HR-MDS with mono- or multihit *TP53* mutation status.

Trial registration: FUSION trial (NCT02775903).

Keywords: AML, gene expression, immune phenotype, MDS, *TP53* mutation

Correspondence to:
Amer M. Zeidan
Section of Hematology, Department of Internal Medicine, Yale University School of Medicine, Yale University, 333 Cedar Street, PO Box 208028, New Haven, CT 06520-8028, USA
amer.zeidan@yale.edu

Jan Philipp Bewersdorf
Section of Hematology, Department of Internal Medicine, Yale University School of Medicine, Yale University, New Haven, CT, USA

Leukemia Service, Department of Medicine, Memorial Sloan Kettering Cancer Center, New York, NY, USA

Vanessa Hasle
Ethan Thompson
Daniel Lopes de Menezes
Shelonidta Rose
Isaac Boss
Brian A. Fox
Bristol Myers Squibb, Princeton, NJ, USA

Rory M. Shallis
Stephanie Halene
Section of Hematology, Department of Internal Medicine, Yale University School of Medicine, Yale University, CT, USA

Torsten Haferlach
MLL Munich Leukemia Laboratory, Munich, Germany

*These authors contributed equally

Introduction

Mutations in *TP53* are found in 10–15% of patients with acute myeloid leukemia (AML) and myelodysplastic syndromes (MDS).[1,2] *TP53* mutations have been associated with increased resistance to conventional cytotoxic chemotherapy and venetoclax-based therapy, and poor survival even after allogeneic hematopoietic cell transplantation.[1,3–5] Although frequently associated with complex karyotypes and dismal

outcomes, recent studies have suggested that *TP53* mutations in AML and higher risk (HR)-MDS are heterogeneous with a variable impact on prognosis.[6–9] The data are conflicting regarding the impact of molecular characteristics of *TP53* mutations such as monoallelic *versus* biallelic mutation status on prognosis, which might be partially due to the differences in patient populations and treatment characteristics of the individual studies.[6,10–13] Recent data also suggest that the prognosis of AML and HR-MDS patients with *TP53* mutations is generally comparable and both could be considered as a single molecularly defined disease entity rather than being classified separately based on blast count.[10,11]

Limited data suggest that *TP53* mutations confer an immunosuppressive phenotype that is characterized by upregulation of programmaed death ligand-1 (PD-L1) expression on hematopoietic stem cells and a higher percentage of immunosuppressive regulatory T-cells, which have been identified as an independent predictor of adverse survival.[14] However, to our knowledge, no studies have assessed the impact of *TP53* allelic status on the immune environment in MDS/AML, and there are limited data correlating *TP53* mutations, but not allelic status, with the epigenetic disease phenotype.[15] A distinct analysis by *TP53* mutant allelic status and other molecular characteristics could help delineate mechanisms contributing to immune escape and ultimately disease relapse.

We have previously reported results of the FUSION AML-001 trial, a large, randomized phase II trial in which 205 patients received azacitidine (AZA) or AZA with the anti-PD-L1 antibody durvalumab in two separate cohorts of older patients with AML or HR-MDS.[16,17] Given the unusually high number of patients with *TP53* mutations in our study ($n = 61$; 29.8%), and the fact that durvalumab did not improve response rates or survival outcomes in either cohort, we have combined patients treated in either treatment arm to assemble one of the largest, highly annotated datasets of *TP53* mutated patients, and compared them to 144 patients with *TP53* wild-type status enrolled in the same study. As clinical outcomes of this patient cohort have been reported separately,[18] this manuscript focuses on the correlative studies describing the molecular,

epigenetic, and immunologic characteristics of *TP53*-mutant AML and MDS.

Methods

Study population
The FUSION trial (NCT02775903) was a randomized, multicenter, open-label, phase II study comparing AZA monotherapy with AZA + durvalumab in previously untreated patients with AML or HR-MDS, who were unfit for intensive chemotherapy. The results of the primary analyses of this trial have previously been published.[16,17] Briefly, adult (≥ 18 years), previously untreated patients with HR-MDS [intermediate, high, or very high risk based on the revised International Prognostic Scoring System (IPSS-R)] or AML (age ≥ 65 years and unfit for intensive chemotherapy) were randomized in a 1:1 ratio to either AZA + durvalumab or AZA monotherapy. Patients received either AZA 75 mg/m^2 subcutaneously during days 1–7 of each 28-day cycle or AZA 75 mg/m^2 subcutaneously during days 1–7 + durvalumab 1500 mg intravenously on day 1 of each 28-day cycle. Treatment was continued until disease progression or occurrence of unacceptable toxicity. As there was no difference in response rates or survival outcomes by treatment arm neither in the overall study population nor among *TP53*-mutated patients and given recent studies reporting similar survival in AML and HR-MDS patients with *TP53* mutations,[10,11] we combined AML and MDS patients independent of treatment assignment for a comparison of *TP53*-mutant and *TP53* wild-type patients. In the trial, overall response rate was defined as a composite of complete remission (CR) and CR with incomplete count recovery among AML patients and as a composite of CR, marrow CR, partial remission, and hematologic improvement among MDS patients in line with International Working Group 2003 and 2006 response criteria, respectively.[19,20] Overall survival (OS) was assessed from the time of randomization in the FUSION trial. Outcomes were assessed every 3 months.

Translational analyses
Mutation profiling. The Munich Leukemia Laboratory (MLL) used a next-generation targeted sequencing assay to assess and characterize gene mutations of samples collected at screening.

Thirty-eight genes were assessed and included those frequently mutated in myeloid malignancies (Supplemental Table 1). The mean sequencing coverage across the panel and samples was approximately 3000x. Genetic alterations not matching the reference sequence were noted as mutated, common single nucleotide polymorphism (SNP), or as a variant of unknown significance (VUS). Mutational load and coverage were assessed at each nonreference location. Only pathogenic *TP53* variants with a variant allele frequency (VAF) ≥2% were included. Patients with a common SNP or VUS in the *TP53* gene were classified as *TP53* wild-type in the analyses comparing *TP53* mutant and *TP53* wild-type patients.

Similar to prior publications,[11,12] we defined multihit *TP53* mutations as any of the following: (I) two or more *TP53* gene variants irrespective of the VAF, (II) at least one *TP53* gene variant co-occurring with a cytogenetic aberration involving chromosome 17p (e.g., abnormality of 17p or monosomy 17), or (III) a single *TP53* mutation with a VAF >55%. For comparisons by allelic state, patients with no mutations or a VUS in *TP53* who had a chromosome 17p abnormality were classified as monohit *TP53* mutations. Based on prior publications, we defined R175H, G245S, R248Q, R248W, R249S, R273C, R273H, and R282W as gain-of-function (GOF) mutations and all other *TP53* mutations as non-GOF.[21]

RNA sequencing. Gene expression profiles of bone marrow (BM) aspirates from screening and cycle 3 day 22 (C3D22) were studied by bulk RNA sequencing.[16,17] EA Genomics (Q2 Solutions) used the Qiagen Micro RNeasy kit (Hilden, Germany) to extract RNA and made libraries using TruSeq SBS v4 chemistry (Illumina, San Diego, USA). Strand specific libraries were prepared by using polyA enrichment and included barcodes. Sequencing was performed on an Illumina HiSeq 2500, with 2×50 bp read lengths. Alignment was performed using a two-pass mode with STAR (v2.5.2b) on the full hg38 human genome, and gene-level counts were obtained using the quantmode GeneCounts option. Gene expression was then normalized with the function voom in the R package limma. Where gene expression is presented in the figures, the data were normalized with voom and log2 transformed, and raw Wilcoxon *p* values shown in plots comparing two groups. The T-cell genes and CD34 were chosen based on *a prior* hypothesis and so the *p* values were not adjusted for multiple testing. Global differential gene expression analysis was performed with limma using a model with the *TP53* mutation status as the term, and the volcano plots show the negative of the log10 of the multiple testing adjusted *p* values (also called the false discovery rate) on the *y*-axis and the log2 of the fold change on the *x*-axis. For gene set enrichment analysis (GSEA), we used the clusterProfiler R package (version 3.14), which uses the R package fGSEA internally and used 1000 permutations to estimate the significance.[22,23] We searched the MSigDB and H (Hallmark) gene sets as provided by the msigdbr R package (version 7.0.1).[22,24] Gene co-expression modules were generated using the baseline samples by taking 6000 genes with the highest standard deviation and calculating all pairwise Pearson correlations followed by module identification using affinity propagation *via* the R package apcluster version 1.4.9.[25,26] The central member of each module was defined as the gene with the highest mean correlation to all the other genes in the module. The central members of each module were treated as nodes, with edges between nodes with a Pearson correlation greater than 0.7 and grouped into communities using a Louvain clustering algorithm and visualized using CanvasXpress.[27] All co-expression module analysis steps were performed interactively using the Gene Atlas software (Needle Genomics, LLC, Seattle, USA). The module expression in van Galen *et al.*[28] (GSE116256) was found by taking the mean expression of all the genes in the module across all the cells of a particular cell type, as labeled in GSE116256.[28]

BM flow cytometry. BM aspirates were collected at screening, C3D22, and C6D22 and sent to MLL for processing and flow cytometry. Two panels of flow cytometry antibodies were used to detect granulocytes, lymphocytes, monocytes, and T-cells and reported as a percent of parent population. Tumor blasts were gated based on CD34 and CD117 variant expression. Surface expression of PD-L1, Programmed death-1 (PD-1), and T-cell immunoglobulin and mucin domain 3 (TIM-3) was assessed on BM cells. PD-L1 (clone 29E.2A3) surface expression was quantified using QuantiBrite Beads (BD Biosciences, New Jersey, USA) and was reported as molecules of equivalent soluble fluorochrome. Data was

analyzed by MLL into a collection of 170 reportable subpopulations in the immune cell and immune checkpoint panel and 68 reportables in the tumor/blast panel.

DNA methylation. DNA methylation of peripheral blood samples was assessed using Illumina's Infinium Human Methylation EPIC methylation array at cycle 1 day 1 (C1D1; pretreatment) and on treatment (C2D1). Functional normalization was used to normalize for interarray technical variation using control probes.[29] ß-values were calculated for each CpG site using the equation $\beta = M/(M + U)$, wherein M and U are the number of methylated and unmethylated probes, respectively. Global DNA methylation scores (GDMSs) were calculated for each sample by counting the number of methylation probes with ß-values greater than 0.7. Changes in median GDMS were calculated by subtracting a patient's C2D1 GDMS from their C1D1 GDMS. Focal DNA demethylation ß-values were analyzed in PD-1, PD-L1, and PD-L2 regulatory regions. A full list of analyzed loci is shown provided in Supplemental Table 2.

Statistical analysis

Survival analysis was performed using the R package 'survival' and 'survminer', with the log-rank p values and median survival shown in the plots. Patient characteristics are compared between patients with mutated *versus* wild-type *TP53* using the 'prop.test' method in R when comparing the proportion of patients in each subgroup (i.e. each row of Table 1), or a Wilcoxon rank sum test for numeric characteristics. All boxplots (box-and-whisker plots) were generated using ggplot2 where the central line shows the median, the ends of the boxes show the interquartile range (IQR) and the whiskers show the most distant point ≤1.5 times the IQR.

Results

Outcomes by TP53 mutation status and treatment assignment

Among the patients with known *TP53* mutation status enrolled in the FUSION trial, 37 had *TP53*-mutated AML, 89 were *TP53* wild-type AML, 24 had *TP53*-mutated HR-MDS, and 55 were *TP53* wild-type HR-MDS patients. We first analyzed OS by treatment assignment (AZA + durvalumab *versus* AZA monotherapy). There was no OS difference between treatment arms neither among AML (median OS 13.0 months for AZA + durvalumab *versus* 14.4 months for AZA monotherapy; $p = 0.20$) nor MDS patients (median OS 11.6 months for AZA + durvalumab *versus* 16.7 months for AZA monotherapy; $p = 0.74$). We next compared OS for patients with *TP53* mutations and those with *TP53* wild-type disease. In the AML cohort, patients with *TP53* mutations had a significantly shorter median OS compared to patients who had *TP53* wild-type disease (median OS 8.1 months *versus* 16.6 months; $p < 0.001$). Similarly, median OS was inferior for *TP53*-mutant MDS patients compared with *TP53* wild-type patients (median OS: 9.8 months *versus* 23.5 months; $p = 0.002$; Supplemental Figure 1). These findings support the rationale for combining patients independent of treatment assignment and disease type (AML *versus* MDS) for further analyses.

Genetic landscape of TP53 mutations

The median VAF for *TP53* mutations was 40%, and 90% had a VAF of ≥10%. The majority (93%) of *TP53* mutations mapped to the p53 DNA-binding domain [Figure 1(a)]. Twelve patients (14.3%) had GOF *TP53* mutations. In terms of *TP53* allelic status, 22 (11.0% of total study population; 36.1% of *TP53*-mutant patients) and 41 (20.5%; 67.2%) patients were classified as monohit and multihit, respectively. Patients with *TP53* mutations had a median of 2 (IQR of 1–2) co-occurring mutations, which was fewer than *TP53* wild-type patients who had a median of 3 (IQR of 2–4) co-occurring mutations [Wilcoxon $p < 0.001$; Figure 1(b) and (c)] with distinct patterns in the distribution of co-occurring mutations [Figure 1(d) and Supplemental Figure 2]. Among patients with *TP53* mutations, no other somatic mutations were detected in 25 patients (42%). Mutations in *SRSF2*, *RUNX1*, and *ASXL1* were enriched in *TP53* wild-type patients compared with *TP53*-mutant patients.

In the AML cohort, patients with *TP53* mutations were more likely to have poor-risk

Table 1. Baseline patient characteristics.

Variable	AML			HR-MDS		
	TP53 mutated (*n* = 37)	*TP53* wild-type (*n* = 89)	*p* Value	*TP53* mutated (*n* = 24)	*TP53* wild-type (*n* = 55)	*p* Value
Median patient age (years; IQR)	75 (72–78)	76 (71.5–81.5)	0.315	74 (69.5–77)	74 (68.5–78)	0.733
Male sex (*N*; %)	20 (54.1%)	48 (53.9%)	1.000	17 (70.8%)	39 (70.9%)	1.000
ECOG (*N*; %)						
0	11 (29.7%)	39 (43.8%)	0.228	7 (29.2%)	25 (45.5%)	0.268
1	22 (59.5%)	46 (51.7%)	0.589	15 (62.5%)	27 (49.1%)	0.394
2	3 (8.1%)	4 (4.5%)	0.715	2 (8.3%)	2 (3.6%)	0.751
Median hemoglobin (g/L; IQR)	89 (84.5–100)	95.5 (86–108)	0.106	90 (81.5–97)	91 (80–99.5)	0.554
Median platelet count ×10⁹/L (IQR)	37 (26.5–60.5)	62.5 (34–97)	0.011	49.5 (25–93)	56 (32.5–99.5)	0.554
Median leukocyte count ×10⁹/L (IQR)	1.77 (1.11–3.32)	2.28 (1.29–3.71)	0.434	3.03 (1.98–4.67)	2.37 (1.50–3.77)	0.131
Median ANC ×10⁹/L (IQR)	0.63 (0.28–1.07)	0.52 (0.26–1.25)	0.880	1.14 (0.79–2.04)	0.96 (0.48–1.81)	0.248
Median bone marrow blasts (%; IQR)	27.5 (21–32)	35.5 (24–56.5)	0.001	7 (5–10)	8.8 (6–15)	0.114
Median peripheral blood blasts (%; IQR)	12 (6–16.5)	12 (4–27)	0.536	3 (2–9.5)	2 (1–4)	0.197
AML WHO classification (*N*; %)				N/A	N/A	N/A
AML-MRC	23 (62.2%)	39 (43.8%)	0.093			
AML, not otherwise categorized	8 (21.6%)	34 (38.2%)	0.112			
AML with gene mutations	1 (2.7%)	5 (5.6%)	0.810			
Therapy-related myeloid neoplasms	4 (10.8%)	1 (1.1%)	0.042			
AML with recurrent genetic abnormalities	0	2 (2.3%)	1.000			
MDS WHO classification (*N*; %)	N/A	N/A	N/A			
RCMD				6 (25.0%)	5 (9.1%)	0.127
RAEB-I				8 (33.3%)	21 (38.2%)	0.875
RAEB-II				6 (25.0%)	23 (41.8%)	0.241
MDS unclassified				0	2 (3.6%)	1.000
MDS/MPN-CMML				0	2 (3.6%)	1.000
Others				4 (16.7%)	2 (3.6%)	1.000
MDS type						
Primary				19 (79.2%)	54 (98.2%)	0.0134
Secondary				5 (20.8%)	1 (18%)	0.0134

(Continued)

Table 1. (Continued)

Variable	AML			HR-MDS		
	TP53 mutated (n = 37)	*TP53* wild-type (n = 89)	*p* Value	*TP53* mutated (n = 24)	*TP53* wild-type (n = 55)	*p* Value
IPSS-R cytogenetic riskclassification (*N*, %)	N/A	N/A	N/A			
Very good				0	2 (3.6%)	1.000
Good				1 (4.2%)	17 (30.9%)	0.021
Intermediate				1 (4.2%)	15 (27.3%)	0.041
Poor				4 (16.7%)	13 (23.6%)	0.692
Very poor				18 (75.0%)	8 (14.6%)	<0.001
IPSS-R (%)	N/A	N/A	N/A			
Intermediate				1 (4.2%)	9 (16.4%)	0.258
High				8 (33.3%)	27 (49.1%)	0.294
Very high				15 (62.5%)	19 (34.6%)	0.039

AML, acute myeloid leukemia; AML-MRC, acute myeloid leukemia -myelodysplasia-related changes; ANC, absolute neutrophil count; CMML – chronic myelomonocytic leukemia; ECOG, Eastern Cooperative Oncology Group; HR-MDS, higher-risk myelodysplastic syndromes; IPSS-R, revised International Prognostic Scoring System; IQR, interquartile range; MDS, myelodysplastic syndrome; MPN, myeloproliferative neoplasm; RAEB, refractory anemia with excess blasts; RCMD, refractory cytopenia with multilineage dysplasia.

cytogenetics (59.5% *versus* 11.2%; $p < 0.001$), therapy-related myeloid neoplasm (10.8% *versus* 1.1%; $p = 0.042$), and lower BM blast percentage (27.5% *versus* 35.5%; $p = 0.001$) compared to *TP53* wild-type. However, there were no statistically significant differences in terms of other baseline demographics and clinical characteristics between *TP53* mutant and *TP53* wild-type patients. Table 1 provides an overview of baseline patient characteristics.

Comparing baseline characteristics of HR-MDS patients (Table 1), patients with *TP53* mutations were statistically significantly more likely to have secondary MDS (20.8% *versus* 1.8%; $p = 0.013$), very poor risk cytogenetics by IPSS-R (75% *versus* 14.6%; $p < 0.001$), and very high risk IPSS-R score (62.5% *versus* 34.6%; $p = 0.039$).

Epigenetic, gene expression, and immunophenotypic landscape of TP53*-mutant and* TP53 *wild-type AML and MDS at baseline*
We analyzed DNA methylation status in peripheral blood samples of AML and HR-MDS patients using the global methylation scores as published previously.[16,17] Global DNA

methylation was independent of *TP53* mutation status at baseline when comparing monohit, multihit, and wild-type patients [*p* value = 0.98 wild-type *versus* monohit; $p = 0.21$ wild-type *versus* multihit; $p = 0.46$ monohit *versus* multihit; Figure 2(a)]. Assessing methylation of PD-1, PD-L1, and PD-L2 gene loci at baseline, we found that especially in PD-L2, various loci showed differences in methylation status depending on *TP53* mutation status (Supplemental Figure 3).

In the BM of AML patients at baseline [Figure 2(b)], $CD3^+$ T-cell and PD-L1-positive $CD34^+$ progenitor cell percentages were statistically significantly higher in *TP53*-mutated patients, while the myeloid progenitor cell percentage (all as a percent of total cells) was higher in *TP53* wild-type patients. However, these differences were not present in MDS patients [Figure 2(c)]. Additionally, AML patients with *TP53* mutations had a higher abundance of exhausted T-cells [$CD3^+CD8^+PD1^+TIM3^-$ T-cells ($p = 0.033$) and $CD3^+CD8^+PD1^-TIM3^+$ T-cells ($p = 0.008$); each as percentage of total cells] compared to *TP53* wild-type AML patients (plot not shown; and $p > 0.05$ in MDS). When analyzing the pooled
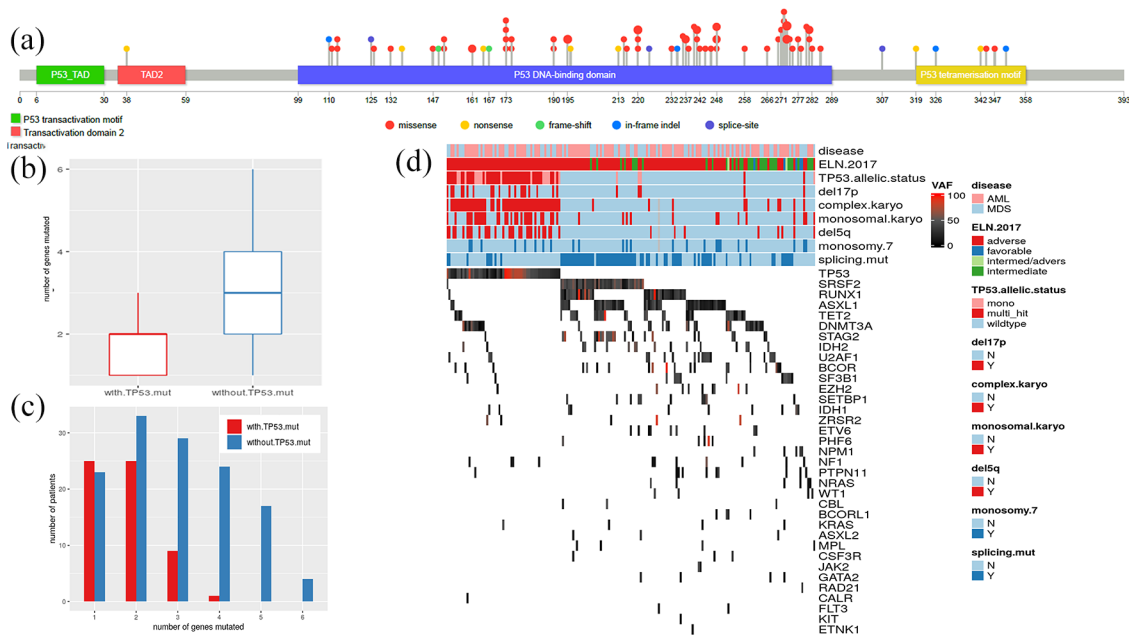
Figure 1. *TP53* and co-occurring mutations. Panel (a) Illustrates the distribution and type of *TP53* mutations as a lollipop plot. The majority of *TP53* mutations were missense mutations localized in the p53 DNA-binding domain. Patients with *TP53* mutations had a lower number of co-occurring mutations compared to *TP53* wild-type patients (b; the central line shows the median, the ends of the boxes show the interquartile range (IQR) and the whiskers show the most distant point ⩽1.5 times the IQR). *TP53* mutations occurred in isolation in 41.7% of patients, while *TP53* wild-type patients frequently had several co-occurring mutations (c). The mutational and cytogenetic patterns by *TP53* mutational status are shown in panel (d).

cohort of AML and HR-MDS by *TP53* mutation status, patients with *TP53* mutations had higher median levels of PD-L1-positive, CD34$^+$ progenitors (5.6% *versus* 2.4%; $p = 0.006$) and fewer myeloid progenitor cells (58% *versus* 75%; $p = 0.005$) than *TP53* wild-type patients [Figure 2(d)].

To evaluate differences in gene expression profile by *TP53* mutation status, we conducted bulk RNA sequencing of baseline BM aspirates (24 *TP53* mutant and 84 *TP53* wild-type). In the baseline samples, the number of differentially expressed genes (DEGs) between *TP53*-mutant samples and *TP53* wild-type samples was higher in the AML cohort (1887 genes) compared to the HR-MDS cohort (78 genes) (Supplemental Figure 4 and Supplemental Table 3). DEGs from our cohort overlapped significantly with an independent dataset of *TP53*-mutant *versus TP53* wild-type AML samples from the Beat AML cohort (Supplemental Figure 5), supporting the validity of our findings. Patterns of DEGs were similar for multihit *TP53* mutations *versus* wild-type as they were for all *TP53* mutations *versus*

wild-type. The gene which had the largest difference in expression in *TP53*-mutant samples relative to *TP53* wild-type samples was *ZNF560*. Additionally, we found that *TP53*-mutant patients had higher expression of T-cell genes (e.g. IL7R) and markers of proliferation (MKI67) compared to *TP53* wild-type patients (Figure 3). PD-L1 (CD274) expression was also higher in *TP53*-mutant patients compared to wild-type among both AML and HR-MDS patient cohorts.

To infer which cell subsets were underlying these differences in gene expression, we generated co-expression modules of the 6000 genes with the highest standard deviation and calculated the fold change of the central gene of each module by *TP53* mutation status (*TP53* mutant *versus* wild-type). Using previously published single-cell RNA sequencing (scRNA-seq) data from BM cells of AML patients and healthy subjects as a reference,[28] we mapped the co-expression modules to individual cell compartments. We found that modules with higher expression in T-cells (central genes: *BCL11B*, *TBX21*, *SPOCK2*,
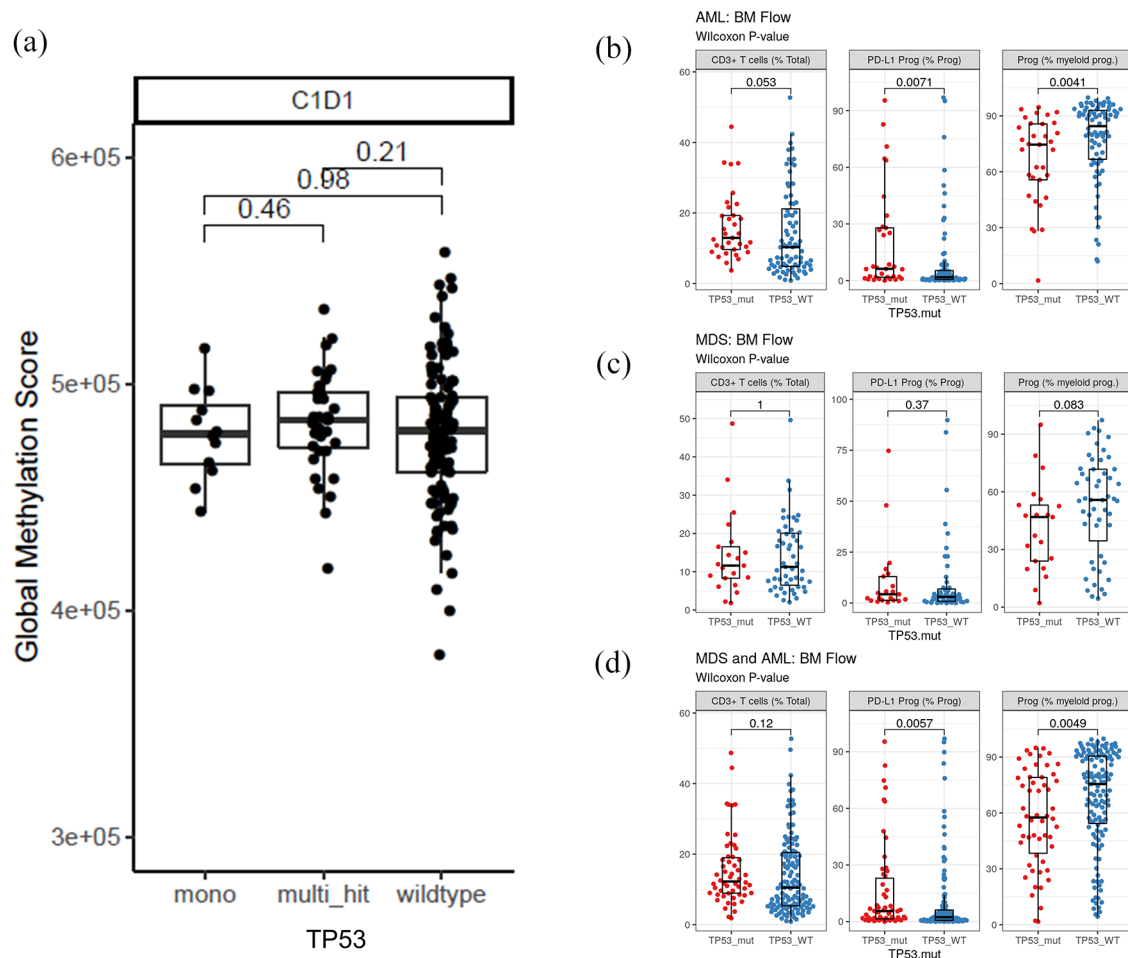
Figure 2. Baseline global DNA methylation status and immune phenotype by *TP53* mutation status. Panel (a) shows the global DNA methylation score at baseline without statistically significant differences between *TP53* wild-type, monohit or multihit *TP53*-mutant patients. Global DNA methylation score is shown as box-and-whisker plots with median and interquartile range. Distribution by *TP53* mutation status was compared using Wilcoxon rank sum test. Figure panels (b–d) show flow cytometry from baseline bone marrow samples for AML patients (b), HR-MDS patients (c), and the combined patient cohort (d) by *TP53* mutation status, respectively. Box-and-whisker plots show the median and interquartile range. Distribution by *TP53* mutation status was compared using Wilcoxon rank sum test.
AML, acute myeloid leukemia; HR-MDS, higher-risk myelodysplastic syndromes.

SIT1, *SLFN12L*, *PLEKHA1*) and myeloid cells (central genes: *LILRB3*, *CKAP4*, *ANXA3*, *COL17A1*, *NFAM1*, *SNX18P8*) demonstrated higher expression in *TP53*-mutant compared to *TP53* wild-type samples (Figure 4), corroborating the T-cell specific single genes selected and shown as examples in Figure 3. Additionally, another community of modules was higher in *TP53*-mutated samples and were more highly expressed in the early and late erythroid cell clusters from van Galen *et al.*[28] Some of those erythroid related modules had genes involved in cell cycle regulation (e.g. *SPTB*, *TOP2A*, *SLC22A23*, *DNAJC6*).

Interestingly, the differential expression of cell cycle genes mapped to progenitor cell types and late erythroid precursors likely reflecting the tumor cell compartment.

Finally, we conducted GSEA of the combined AML and HR-MDS DEGs and found enrichment of genes in the hallmark gene sets of heme metabolism, inflammatory response, cell cycle regulation (e.g. G2M checkpoint, mitotic spindle, and E2F targets), and transforming growth factor-β signaling pathways in *TP53*-mutant patients.[24] Conversely, oxidative
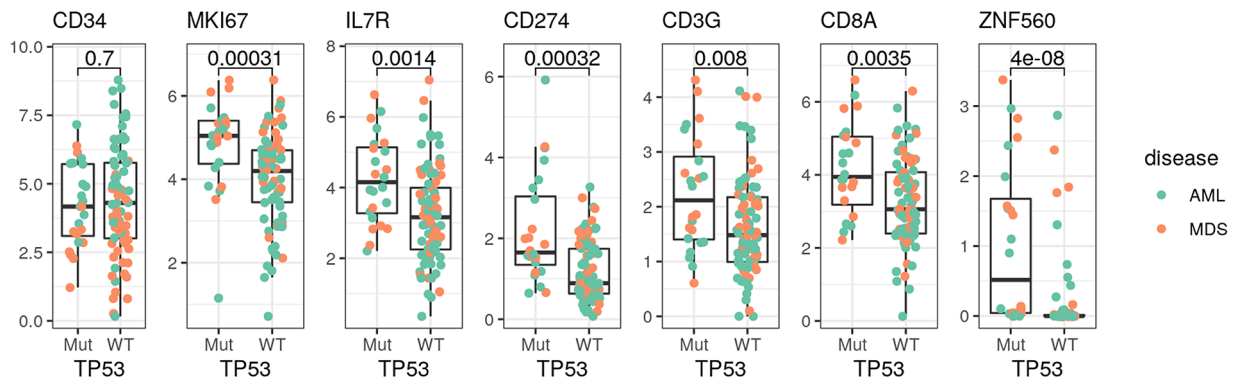
Figure 3. Gene expression pattern by *TP53* mutation status in screening samples. Figure shows genes with statistically significant RNA expression levels with higher expression in *TP53*-mutant patients. *TP53*-mutant patients had higher expression of T-cell genes (e.g. IL7R), markers of proliferation (MKI-67), PD-L1 (CD274) expression compared to wild-type. Differences in gene expression between *TP53*-mutant and *TP53* wild-type samples applied to both AML and HR-MDS patient cohorts. Box-and-whisker plots show the median and interquartile range. Distribution by *TP53* mutation status was compared using Wilcoxon rank sum test. AML, acute myeloid leukemia; HR-MDS, higher-risk myelodysplastic syndromes.

phosphorylation, interferon (IFN)-α, and *MYC* target genes were enriched in *TP53* wild-type patients (Supplemental Figure 6).

Epigenetic, gene expression, and immunophenotypic landscape of TP53-*mutant and* TP53 *wild-type AML and HR-MDS following treatment with AZA and durvalumab*

To evaluate for any differences in epigenetic, gene expression, or immunophenotypic profiles by *TP53* mutation status in response to treatment with AZA ± durvalumab, we analyzed on-treatment samples after one cycle (DNA methylation profile and flow cytometry) or three cycles of treatment (gene expression profile).

In bulk analysis from peripheral blood, AZA led to statistically significant changes in GDMS after one cycle of treatment when compared to baseline across all cohorts but did not differ by *TP53* mutation status (monohit *versus* multihit *versus* wild-type) (Figure 5). When comparing methylation status of specific loci in the PD-1, PD-L1, and PD-L2 genes, all differences in baseline methylation status between multihit *TP53* mutant and *TP53* wild-type samples were reversed on treatment except for two loci of the analyzed PD-L2 gene (cg07211259 and cg11299543) with lower methylation scores in the *TP53* wild-type samples (Supplemental Figure 3).

To evaluate differences in gene expression profiles following treatment with AZA by *TP53* mutation status, we conducted RNA sequencing after three cycles of therapy (27 *TP53* mutant and 97 *TP53* wild-type). When comparing *TP53*-mutant and *TP53* wild-type patients, AML samples had 116 genes, which were differentially expressed while HR-MDS samples had zero DEGs after three cycles of therapy (Supplemental Table 3).

Discussion

In this study, we provide an assessment of the molecular, epigenetic, and immunologic landscape of *TP53*-mutant AML/HR-MDS before and after AZA-based therapy in very well annotated samples from 61 patients with *TP53* mutations and 144 *TP53* wild-type patients who were enrolled in a randomized clinical trial.

One potential mechanism underlying the poor prognosis associated with *TP53* mutations is the induction of an immunosuppressive microenvironment that permits immune evasion of tumor cells.[14,30,31] Supporting this hypothesis, we found higher expression of T-cell-related genes and PD-L1 by RNA sequencing and flow cytometry in pretreatment *TP53*-mutated AML samples compared to pretreatment *TP53* wild-type samples. Of note, these differences were not present
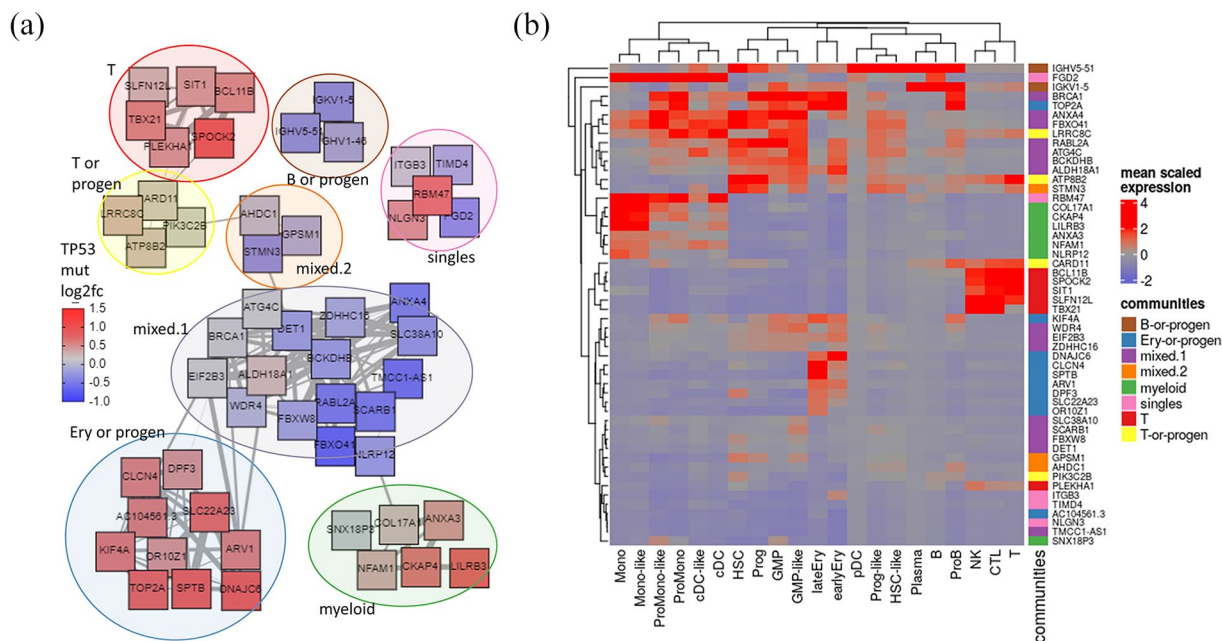
Figure 4. Co-expression modules colored by differential expression in *TP53* mutant *versus* wild-type and projected onto scRNA-seq data from van Galen *et al.*[28] Figure shows the largest 53 co-expression modules from the bulk RNA-seq baseline samples and their logFC in *TP53*-mutant *versus TP53* wild-type and expression in clusters of single cells. In panel (a), each node represents 25–57 genes which are co-expressed and labeled with the most central member of the module. Edges in the network are drawn if the central member has a Pearson correlation greater than or equal to 0.7 to any other node, and the thickness of the line is scaled to the correlation value. The color of each node is the log2 fold change of *TP53* mutant *versus TP53* wild-type with red showing modules which are higher in *TP53*-mutated samples and blue showing the opposite. Communities are shown by circles and defined by the graph structure. The circle labeled 'singles' is a collection of singleton modules, which are not connected to any other modules above a correlation of 0.7. The labels of the remaining communities are from (b), which is a heatmap showing the expression of each co-expression module from (a) in the cell types from the AML and healthy BM scRNA-seq data from van Galen *et al.*[28] (GSE116256). The color of each element in the heatmap is based on the scaled mean of the expression of the genes within each module from (a), and the community names are based on the top cell type labels.

AML, acute myeloid leukemia; BM, bone marrow; scRNA-seq, single-cell RNA sequencing.

in HR-MDS patients. This is in line with prior work showing that PD-L1 expression is increased in MDS and secondary AML BM specimens *via* activation of *MYC*.[14] Recently, AML patients with *TP53* mutations were demonstrated to have higher cytotoxic T-cell and NK-cell infiltration and IFN-γ gene signature.[32] However, it has been previously suggested that immune activation might be balanced by the presence of exhausted cytotoxic T-cells and NK-cells that are characterized by expression of Lymphocyte Activation Gene (LAG-3) and TIM-3.[32] As such, treatment with antibodies targeting LAG-3 and TIM-3 in addition to anti-PD-1 might be more effective in overcoming this immune-exhausted state.[33–35]

The single gene and co-expression module analysis of the RNA sequencing studies showed that genes involved with inflammatory response and

cell cycle regulation were higher in *TP53*-mutant patients compared to wild-type patients. Although we found higher Ki-67 expression in *TP53*-mutant compared with wild-type samples, the reverse was found for BM blast percentage. As our bulk RNA sequencing is limited in terms of distinguishing gene expression on an individual cell level (e.g. tumor *versus* immune cells), it is unclear whether the higher Ki-67 expression was due to differences in blast proliferation or if it reflects a higher rate of turn-over in another cell compartment. Since the blast count in the BM was slightly lower in *TP53*-mutant samples and the gene expression implies that the T-cells and myeloid cells were slightly higher in *TP53*-mutant samples, it seems more likely that the difference in MKI67 gene expression is due to the non-blast cells. Although single-cell analyses were not available in our study to confirm this hypothesis, our
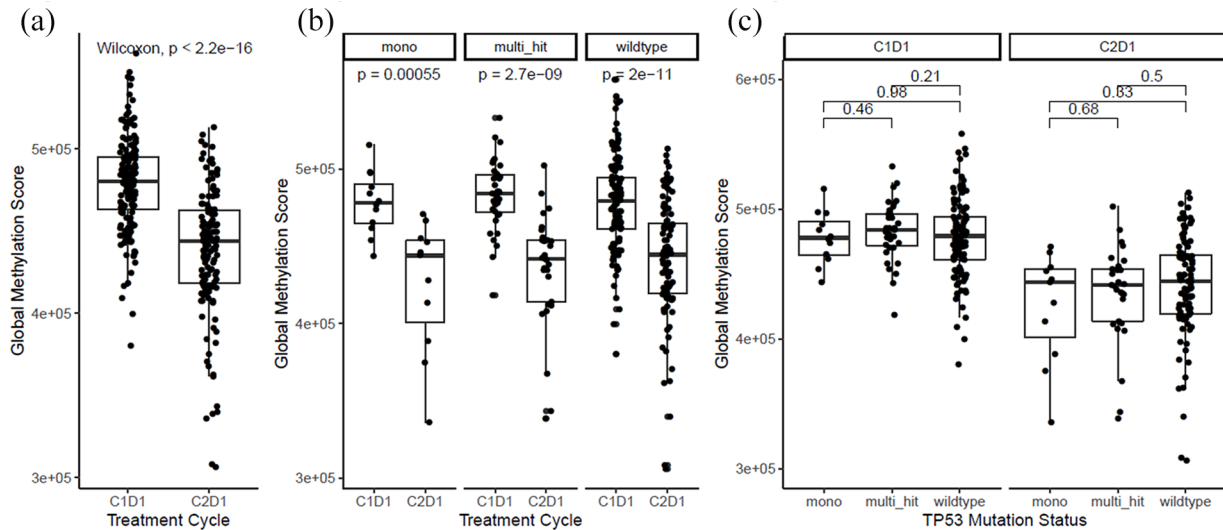
Figure 5. Serial assessment of global DNA methylation status by *TP53* mutation status. Figure shows the global DNA methylation score at baseline and after one cycle of treatment with azacitidine ± durvalumab for all patients (a). Patients experienced a decline in global DNA methylation scores independent of *TP53* mutation status (b) without statistically significant differences between *TP53* wild-type, monohit or multihit *TP53*-mutant patients neither at baseline nor after one cycle of treatment (c). This supports that HMAs exert an objective pharmacodynamic effect in patients independent of *TP53* mutation status. Global DNA methylation score is shown as box-and-whisker plots with median and interquartile range. Distribution by *TP53* mutation status was compared using Wilcoxon rank sum test.
HMA, hypomethylating agent.

observations are also supported by a recent study using single-cell multiomics of hematopoietic stem/progenitor cells from patients with *TP53*-mutant post-MPN AML.[36] Another study using data from the Cancer Genome Atlas (TCGA) and BeatAML cohorts showing an increase in CD8^{+} T-cells and upregulation of immune response signaling pathways in *TP53*-mutant AML patients.[37] The role of other DEGs in *TP53*-mutant AML and HR-MDS warrants additional studies although some of the genes identified in our analysis such as *ZNF560* have been implicated in ferroptosis and potentially confer an adverse prognosis in AML.[38]

Treatment with hypomethylating agents (HMAs) has been shown to lead to an upregulation of PD-1 and PD-L1 in preclinical models of AML, which suggested a potential synergy of combined treatment with HMA and anti-PD-L1 antibodies.[39] With data demonstrating an higher expression of PD-1/PD-L1 in patients with *TP53* mutations compared to wild-type, this combination might be especially effective in such patients.[14,40] However, the negative findings of the FUSION trial and *post hoc* analyses of

TP53-mutant patients suggest that targeting PD-L1 might not be clinically useful in AML and HR-MDS.[16–18] As a pharmacodynamic surrogate, we found that changes in the GDMSs with AZA treatment were similar in *TP53*-mutant and *TP53* wild-type patients supporting that AZA may have equal pharmacodynamic effects in *TP53*-mutant patients, and that these changes are insufficient to overcome the adverse prognosis of *TP53* mutations. While the specific epigenetic changes induced by HMA are poorly characterized, and the tumor cells were not a majority cell type in the bulk cells of peripheral blood, there were several differences in methylation of various loci in the genes for PD-1, PD-L1, and PD-L2 in patients with *TP53* mutations *versus TP53* wild-type patients. Although the functional implications of most of the variably methylated loci are largely unknown, changes in methylation patterns that lead to upregulation of immune checkpoint receptors could potentially contribute to resistance to HMA ± immune checkpoint inhibitors.

The role of myeloid immune checkpoints in myeloid malignancies has received increasing attention recently.[41] Leukocyte immunoglobulin-like

receptor B-3 (LILRB3) is exclusively expressed on myeloid cells and its activation has recently been associated with enhanced leukemic cell survival and inhibition of T cell-mediated anti-tumor activity.[42] In our analyses, we found that LILRB3 expression was statistically significantly higher among *TP53*-mutant patients and mapped to the myeloid compartment, which includes both normal myeloid cells and potential tumor cells, suggesting that the immunosuppressive effects of *TP53* mutations are not limited to the anti-tumor T-cell immune function and that inhibitory myeloid immune checkpoints such as LILRB3 might constitute another therapeutic target.[43] Preclinical studies have already demonstrated the anti-leukemic effect of LILRB3-blocking antibodies in several AML xenograft models.[42] Although different members of the LILRB family have distinct biologic functions, LILRB4 has also been shown to mediate T-cell suppression in AML models and clinical trials targeting LILRB4 are already ongoing (NCT04372433).[44,45]

Potential limitations of our study include the smaller sample size compared to other studies and the pooling of treatment and disease entities. However, as the outcomes, baseline characteristics, and most immunophenotypic and molecular analyses of AML and HR-MDS patients as well as treatment group (AZA + durvalumab *versus* AZA monotherapy) were comparable, the effect of this pooled analysis is unlikely to affect the main conclusions of our study. While our power to detect small differences was limited by sample size, the potential benefits of using samples collected as part of a randomized clinical trial reduce the risk of confounding by treatment, patient, and disease characteristics that might have affected prior studies. As our analyses were performed on samples from clinical trial patients, the extent of the analyses was limited by sample availability and research methods available. Future studies using single-cell sequencing technologies instead of bulk RNA sequencing will be important to decipher the impact of specific immune cell subsets. Additionally, integration with other research methodologies to evaluate other aspects of the underlying disease biology such as ATAC-seq to evaluate chromatin accessibility and proteomic studies can be informative to derive a more comprehensive understanding of *TP53*-mutant AML/MDS. However, these studies were beyond the scope of this manuscript.

In summary, we present the largest comprehensive molecular, epigenetic, and immune-phenotypical characterization of AML and HR-MDS patients with *TP53* mutations treated with HMA-based therapy in a clinical trial. Upregulation of inhibitory immune checkpoints such as PD-1 and notably the myeloid immune checkpoint LILRB3 could be contributing to the poor prognosis and frequent disease relapse *via* immune escape.

Declarations

Author contributions
Amer M. Zeidan: Conceptualization; Data curation; Funding acquisition; Investigation; Project administration; Supervision; Writing – review & editing.

Jan Philipp Bewersdorf: Conceptualization; Formal analysis; Writing – original draft; Writing – review & editing.

Vanessa Hasle: Formal analysis; Investigation; Writing – review & editing.

Rory M. Shallis: Investigation; Writing – review & editing.

Ethan Thompson: Conceptualization; Formal analysis; Writing – review & editing.

Daniel Lopes de Menezes: Conceptualization; Formal analysis; Writing – review & editing.

Shelonitda Rose: Investigation; Writing – review & editing.

ORCID iDs
Amer M. Zeidan https://orcid.org/0000-0001-7017-8160

Jan Philipp Bewersdorf https://orcid.org/0000-0003-3352-0902

Rory M. Shallis https://orcid.org/0000-0002-8542-2944

References

1. Haferlach T, Nagata Y, Grossmann V, *et al.* Landscape of genetic lesions in 944 patients with myelodysplastic syndromes. *Leukemia* 2014; 28: 241–247.

2. Cancer Genome Atlas Research Network, Ley TJ, Miller C, *et al.* Genomic and epigenomic landscapes of adult de novo acute myeloid leukemia. *N Engl J Med* 2013; 368: 2059–2074.

3. Jadersten M, Saft L, Smith A, *et al.* TP53 mutations in low-risk myelodysplastic syndromes with del(5q) predict disease progression. *J Clin Oncol* 2011; 29: 1971–1979.

4. Bejar R, Stevenson K, Abdel-Wahab O, *et al.* Clinical effect of point mutations in myelodysplastic syndromes. *N Engl J Med* 2011; 364: 2496–2506.

5. Lindsley RC, Saber W, Mar BG, *et al.* Prognostic mutations in myelodysplastic syndrome after stem-cell transplantation. *N Engl J Med* 2017; 376: 536–547.

6. Bernard E, Nannya Y, Hasserjian RP, *et al.* Implications of *TP53* allelic state for genome stability, clinical presentation and outcomes in myelodysplastic syndromes. *Nat Med* 2020; 26: 1549–1556.

7. Haase D, Stevenson KE, Neuberg D, *et al.* *TP53* mutation status divides myelodysplastic syndromes with complex karyotypes into distinct prognostic subgroups. *Leukemia* 2019; 33: 1747–1758.

8. Boettcher S, Miller PG, Sharma R, *et al.* A dominant-negative effect drives selection of *TP53*

missense mutations in myeloid malignancies. *Science* 2019; 365: 599–604.

9. Kanagal-Shamanna R, Montalban-Bravo G, Katsonis P, *et al*. Evolutionary action score identifies a subset of TP53 mutated myelodysplastic syndrome with favorable prognosis. *Blood Cancer J* 2021; 11: 52.

10. Weinberg OK, Siddon A, Madanat YF, *et al*. *TP53* mutation defines a unique subgroup within complex karyotype de novo and therapy-related MDS/AML. *Blood Adv* 2022; 6: 2847–2853.

11. Grob T, Al Hinai ASA, Sanders MA, *et al*. Molecular characterization of mutant *TP53* acute myeloid leukemia and high-risk myelodysplastic syndrome. *Blood*. 2022; 139: 2347–2354.

12. Zeidan A, Bewersdorf J, Hasle V, *et al*. Prognostic Implications of Mono-Hit and Multi-Hit TP53 Alterations in Patients with Acute Myeloid Leukemia and Higher Risk Myelodysplastic Syndromes Treated with Azacitidine-based Therapy. *Leukemia*. 2022; In press.

13. Short NJ, Montalban-Bravo G, Hwang H, *et al*. Prognostic and therapeutic impacts of mutant *TP53* variant allelic frequency in newly diagnosed acute myeloid leukemia. *Blood Adv* 2020; 4: 5681–5689.

14. Sallman DA, McLemore AF, Aldrich AL, *et al*. *TP53* mutations in myelodysplastic syndromes and secondary AML confer an immunosuppressive phenotype. *Blood*. 2020; 136: 2812–2823.

15. Wang W, Auer P, Zhang T, *et al*. Impact of epigenomic hypermethylation at *TP53* on allogeneic hematopoietic cell transplantation outcomes for myelodysplastic syndromes. *Transplant Cell Ther* 2021; 27: 659.e1–659.e6.

16. Zeidan AM, Boss I, Beach CL, *et al*. A randomized phase 2 trial of azacitidine with or without durvalumab as first-line therapy for higher-risk myelodysplastic syndromes. *Blood Adv* 2022; 6: 2207–2218.

17. Zeidan AM, Boss I, Beach CL, *et al*. A randomized phase 2 trial of azacitidine with or without durvalumab as first-line therapy for older patients with AML. *Blood Adv* 2022; 6: 2219–2229.

18. Zeidan AM, Bewersdorf JP, Hasle V, *et al*. Prognostic implications of mono-hit and multi-hit *TP53* alterations in patients with acute myeloid leukemia and higher risk myelodysplastic syndromes treated with azacitidine-based therapy. *Leukemia*. 2023; 37: 240–243.

19. Cheson BD, Bennett JM, Kopecky KJ, *et al*. Revised recommendations of the International Working Group for Diagnosis, Standardization of Response Criteria, Treatment Outcomes, and Reporting Standards for Therapeutic Trials in Acute Myeloid Leukemia. *J Clin Oncol* 2003; 21: 4642–4649.

20. Cheson BD, Greenberg PL, Bennett JM, *et al*. Clinical application and proposal for modification of the International Working Group (IWG) response criteria in myelodysplasia. *Blood* 2006; 108: 419–425.

21. Roszkowska KA, Piecuch A, Sady M, *et al*. Gain of function (GOF) mutant p53 in cancer – current therapeutic approaches. *Int J Mol Sci*. 2022; 23: 13287.

22. Subramanian A, Tamayo P, Mootha VK, *et al*. Gene set enrichment analysis: a knowledge-based approach for interpreting genome-wide expression profiles. *Proc Natl Acad Sci U S A* 2005; 102: 15545–15550.

23. Korotkevich G, Sukhov V and Sergushichev A. Fast gene set enrichment analysis. *bioRxiv*. 2019.

24. Liberzon A, Birger C, Thorvaldsdóttir H, *et al*. The Molecular Signatures Database (MSigDB) hallmark gene set collection. *Cell Syst* 2015; 1: 417–425.

25. Bodenhofer U, Kothmeier A and Hochreiter S. APCluster: an R package for affinity propagation clustering. *Bioinformatics* 2011; 27: 2463–2464.

26. Frey BJ and Dueck D. Clustering by passing messages between data points. *Science* 2007; 315: 972–976.

27. Neuhaus, I. *CanvasXpress: a JavaScript library for data analytics with full audit trail capabilities*. https://canvasxpress.org/

28. van Galen P, Hovestadt V, Wadsworth Ii MH, *et al*. Single-cell RNA-Seq reveals AML hierarchies relevant to disease progression and immunity. *Cell*. 2019; 176: 1265–1281.e24.

29. Fortin JP, Labbe A, Lemire M, *et al*. Functional normalization of 450k methylation array data improves replication in large cancer studies. *Genome Biol* 2014; 15: 503.

30. Vadakekolathu J, Lai C, Reeder S, *et al*. *TP53* abnormalities correlate with immune infiltration and associate with response to flotetuzumab immunotherapy in AML. *Blood Adv* 2020; 4: 5011–5024.

31. Williams P, Basu S, Garcia-Manero G, *et al*. The distribution of T-cell subsets and the expression of immune checkpoint receptors and ligands in

patients with newly diagnosed and relapsed acute myeloid leukemia. *Cancer* 2019; 125: 1470–1481.

32. Dufva O, Pölönen P, Brück O, *et al.* Immunogenomic landscape of hematological malignancies. *Cancer Cell.* 2020; 38: 380–399.e13.

33. Bewersdorf JP, Shallis RM and Zeidan AM. Immune checkpoint inhibition in myeloid malignancies: moving beyond the PD-1/PD-L1 and CTLA-4 pathways. *Blood Rev* 2020; 45: 100709.

34. Wolf Y, Anderson AC and Kuchroo VK. TIM3 comes of age as an inhibitory receptor. *Nat Rev Immunol* 2020; 20: 173–185.

35. Abdelhakim H, Cortez LM, Li M, *et al.* LAG3 Inhibition decreases AML-induced immunosuppression and improves T cell-mediated killing. *Blood* 2019; 134: 3605-.

36. Rodriguez-Meira A, Norfo R, Wen S, *et al.* Single-cell multi-omics identifies chronic inflammation as a driver of *TP53*-mutant leukemic evolution. *Nat Genet* 2023; 55: 1531–1541.

37. Wen X-M, Xu Z-J, Jin Y, *et al.* Association analyses of *TP53* mutation with prognosis, tumor mutational burden, and immunological features in acute myeloid leukemia. *Front Immunol* 2021; 12: 717527.

38. Wang J, Zhuo Z, Wang Y, *et al.* Identification and validation of a prognostic risk-scoring model based on ferroptosis-associated cluster in acute myeloid leukemia. *Front Cell Dev Biol* 2022; 9: 800267-.

39. Yang H, Bueso-Ramos C, DiNardo C, *et al.* Expression of PD-L1, PD-L2, PD-1 and CTLA4 in myelodysplastic syndromes is enhanced by treatment with hypomethylating agents. *Leukemia* 2014; 28: 1280–1288.

40. Zajac M, Zaleska J, Dolnik A, *et al.* Expression of CD274 (PD-L1) is associated with unfavourable recurrent mutations in AML. *Br J Haematol* 2018; 183: 822–825.

41. Abaza Y and Zeidan AM. Immune checkpoint inhibition in acute myeloid leukemia and myelodysplastic syndromes. *Cells* 2022; 11: 2249.

42. Wu G, Xu Y, Schultz RD, *et al.* LILRB3 supports acute myeloid leukemia development and regulates T-cell antitumor immune responses through the TRAF2-cFLIP-NF-κB signaling axis. *Nat Cancer* 2021; 2: 1170–1184.

43. Yeboah M, Papagregoriou C, Jones DC, *et al.* LILRB3 (ILT5) is a myeloid cell checkpoint that elicits profound immunomodulation. *JCI Insight* 2020; 5: e141593.

44. Deng M, Gui X, Kim J, *et al.* LILRB4 signalling in leukaemia cells mediates T cell suppression and tumour infiltration. *Nature* 2018; 562: 605–609.

45. Li Z, Deng M, Huang F, *et al.* LILRB4 ITIMs mediate the T cell suppression and infiltration of acute myeloid leukemia cells. *Cell Mol Immunol* 2020; 17: 272–282.

Visit Sage journals online
journals.sagepub.com/
home/tah

S Sage journals